Enhanced Illumination Sensing Using Multiple Harmonics for LED Lighting Systems

Hongming Yang, *Member, IEEE*, Tim C. W. Schenk, *Member, IEEE*, Jan W. M. Bergmans, *Senior Member, IEEE*, and Ashish Pandharipande, *Senior Member, IEEE*

***Abstract*—This paper considers frequency division multiplexing (FDM) based illumination sensing in light emitting diode (LED) lighting systems. The purpose of illumination sensing is to identify the illumination contributions of spatially distributed LEDs at a sensor location, within a limited response time. In the FDM scheme, LEDs render periodical illumination pulse trains at different frequencies with prescribed duty cycles. The problem of interest is to estimate the amplitudes of the individual illumination pulse trains. In our previous work, an estimation approach was proposed using the fundamental frequency component of the sensor signal. The number of LEDs that can be supported by this estimation approach is limited to around 100 LEDs at a response time of 0.1 s. For future LED lighting systems, however, it is desirable to support many more LEDs. To this end, in this paper, we seek to exploit multiple harmonics in the sensor signal. We first derive upper limits on the number of LEDs that can be supported in the presence of frequency offsets and noise. Thereafter, we propose a low complexity successive estimation approach that effectively exploits the multiple harmonics. It is shown that the number of the LEDs can be increased by a factor of at least five, compared to the estimation approach using only the fundamental frequency component, at the same estimation error.**

***Index Terms*—Cramér–Rao bound, frequency division multiplexing, illumination sensing, light emitting diode lighting systems, successive estimation.**

I. Introduction

LIGHT emitting diodes (LEDs) will largely replace incandescent and fluorescent lamps in the next few years. Besides energy efficiency, one of the key advantages of LED lighting systems is their ability to render colorful, dynamic and localized lighting effects [1], [2]. This ability results mainly from three factors. First, LEDs are colored light sources by nature. Secondly, each LED can provide hundreds of perceived illumination levels through pulse width modulation (PWM) dimming [3]. Finally, an LED lighting system normally consists of a large number of spatially distributed LEDs with narrow light beams. These three factors create many degrees of freedom to render appealing lighting effects. Consequent to these factors, a key technical challenge, however, occurs in the control of such lighting systems.

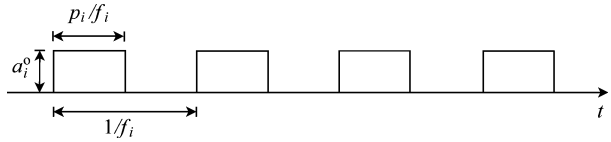

Fig. 1. Illustration of the received optical signal due to the ith LED. The amplitude of the corresponding electrical pulse train is a_i.

In order to tackle this challenge, the concept of illumination sensing was proposed in [4]. In this concept, the illumination pulses emitted by different LEDs are modulated differently. A sensor is then placed at the target location where a certain lighting effect is desired. The role of this sensor and associated sensor signal processing is to distinguish and estimate the illumination contribution of each LED. Based on the estimation results, a central controller can determine the setting of the duty cycle for each individual LED to achieve the desired lighting effect.

More specifically, due to PWM dimming, each LED renders a periodical optical pulse train with prescribed duty cycle. A typical received optical signal from the ith LED with frequency f_i is illustrated in Fig. 1. The amplitude of the pulse train is called the *illuminance* (in lumen/m^2, or lux), denoted by $a_i^{\rm o}$, and the duty cycle is denoted by p_i where $0 \leq p_i \leq 1$. The illumination contribution of the LED at the target location is given by the product $a_i^{\rm o} p_i$. The duty cycle p_i is known from the controller. The amplitude $a_i^{\rm o}$ is determined by the radiation pattern of the ith LED [5] and the free-space optical channel attenuation [6], and is unknown. The key challenge for illumination sensing is then to distinguish the signals from different LEDs and estimate $a_i^{\rm o}$ for each i to determine the illumination contribution of the ith LED. Moreover, due to practical application requirements [7], the estimation process has to be performed with a high accuracy and within a limited response time, e.g., $T < 0.1$ s, as will be explained in more detail in Section II.

The optical signals from all the LEDs superimpose at the target location. It is difficult and expensive, if not impossible, to distinguish different LEDs optically. Therefore, the received optical signal is converted into an electrical signal, namely *sensor signal*, by using a photosensor, such as a photodiode. The amplitude of the electrical pulse train is then denoted by a_i. Provided

Manuscript received November 28, 2009; accepted June 19, 2010. Date of publication July 26, 2010; date of current version October 13, 2010. The associate editor coordinating the review of this manuscript and approving it for publication was Prof. Maciej Niedzwiecki. The material in this paper was presented in part at the 2010 IEEE International Conference on Acoustics, Speech, and Signal Processing (ICASSP), Dallas, TX, 2010.

H. Yang was with the Department of Electrical Engineering, Eindhoven University of Technology, Eindhoven, The Netherlands. He is now with the Department of Distributed Sensor Systems, Philips Research Eindhoven, 5656 AE Eindhoven, The Netherlands (e-mail: hongming.yang@philips.com).

T. C. W. Schenk and A. Pandharipande are with the Department of Distributed Sensor Systems, Philips Research Eindhoven, 5656 AE Eindhoven, The Netherlands (e-mail: tim.schenk@philips.com; ashish.p@philips.com).

J. W. M. Bergmans is with the Department of Electrical Engineering, Eindhoven University of Technology, 5600 MB Eindhoven, The Netherlands (e-mail: J.W.M.Bergmans@tue.nl).

Color versions of one or more of the figures in this paper are available online at http://ieeexplore.ieee.org.

Digital Object Identifier 10.1109/TSP.2010.2059018

that the sensitivity of the photodiode is accurately known, the challenge of illumination sensing is thus transformed into the estimation of a_i. To this end, one may consider modulating the illumination waveform in Fig. 1 differently for each LED such that the signals can be disentangled electronically at the sensor.

With respect to the modulation method, various approaches have been proposed [4], [7], [8]. In this paper, we focus on the method of frequency division multiplexing (FDM) [8], since this method does not require synchronism among the spatially distributed LEDs. In this method, the frequencies $\{f_i\}$ of the illumination pulse trains are used as the identifiers of different LEDs. Therefore, these $\{f_i\}$ are set to be different, with a discernible spacing, denoted by Δ_f, between adjacent frequencies. Note that these $\{f_i\}$ are all chosen within a frequency range, usually between 2 kHz and 4 kHz [7], which is determined mainly by the requirement of no visible flicker and by optical properties such as the on- and off-switch response time of the LEDs.

Based on the FDM scheme, a simple estimator was proposed in [7] which only uses the fundamental frequency component of the sensor signal. The basic idea was to estimate a_i based on the value of the Fourier transform of the sensor signal at the frequencies f_i. The sensor signal $y(t)$ can be written as $y(t) = \sum_i y_i(t) + v(t)$, where $y_i(t)$ is the sensor signal component due to the ith LED and $v(t)$ denotes the noise. In a practical application scenario, the effect of noise on this estimation performance is negligible due to the high signal-to-noise ratio (SNR). Instead, the performance of such an estimator is mainly affected by three other factors:

1) Response Time: Due to the required limited response time T, a windowing function $g(t)$, e.g., a triangular function, with limited time span T, needs to be applied to $y(t)$ before the Fourier transform is taken. Let $Y(f)$ denote the result of the Fourier transform, i.e., $Y(f) = \mathcal{F}[y(t)g(t)]$, where $\mathcal{F}[\cdot]$ denotes the Fourier transform. Hence, we have

$$\begin{aligned} Y(f) &= \sum_i \mathcal{F}[y_i(t)g(t)] + \mathcal{F}[v(t)g(t)] \\ &= \sum_i \bar{Y}_i(f) * G(f) + V(f) * G(f) \end{aligned} \tag{1}$$

where $\bar{Y}_i(f) = \mathcal{F}[y_i(t)]$, $G(f) = \mathcal{F}[g(t)]$, $V(f) = \mathcal{F}[v(t)]$, and '$*$' denotes convolution. Due to the periodic nature of the signal $y_i(t)$, $\bar{Y}_i(f)$ contains line spectra at $\{mf_i\}$, where m is an integer. However, with the spectrum widening due to the windowing function, $Y(f)$ contains the weighted sum of $G(f - mf_i)$ for all i and m. These functions $\{G(f - mf_i)\}$ might overlap each other in the frequency domain. As a consequence, $Y(f_i)$ contains not only the component from the ith LED, but also components from other LEDs, especially those with adjacent frequencies. This influence on the value of $Y(f_i)$ due to other LEDs than the ith LED, can be viewed as interference induced in the sensor signal processing, and is named *induced interference* in this paper. The estimation accuracy of a_i based on $Y(f_i)$ is thus limited by this induced interference. Since the interference level is mainly determined by the windowing function, one may consider to reduce the interference through optimization of the windowing function, as was done in [7].

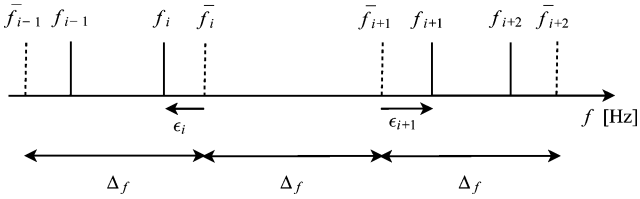

Fig. 2. Illustration of frequency offsets.

2) Frequency Offsets: Due to clock inaccuracies, the LEDs may not be operated precisely at the ideally assigned frequencies. Let $\bar{f}_i$ denote the assigned frequency of the ith LED, f_i the actual frequency and ϵ_i the frequency offset, i.e., $\epsilon_i = f_i - \bar{f}_i$. Fig. 2 illustrates the effect of frequency offsets. Even if $\{\bar{f}_i\}$ are assigned such that there is a uniform spacing Δ_f between adjacent frequencies, the actual spacing $\Delta'_{f,i} = f_{i+1} - f_i = \Delta_f + \epsilon_{i+1} - \epsilon_i$ is normally different from Δ_f and the value is also different for different i. The induced interference is dependent on the actual frequencies $\{f_i\}$, which are unknown. Specifically, the induced interference from the $(i+1)$th LED to the ith LED at $Y(f_i)$ is proportional to $G(f_{i+1} - \bar{f}_i) = G(\Delta_f + \epsilon_{i+1})$. Hence the existence of frequency offsets makes it more difficult to control the induced interference through the optimization of $G(f)$.

3) Duty Cycles: The estimation performance deteriorates when the power of the fundamental frequency component is small, e.g., when p_i is close to 0 or 1, because the induced interference from other LEDs then gives a relatively larger impact on the estimation of a_i.

Due to these reasons, as shown in [7], we have (through setting the value Δ_f to be sufficiently large, e.g., $\Delta_f \geq 2/T$) to make the value of $\Delta_f + \epsilon_{i+1}$ large enough in order to limit the induced interference in the presence of frequency offsets. Given a fixed frequency range for the allocation of $\{\bar{f}_i\}$, the number of LEDs that can be supported is thus limited. Specifically, the number of LEDs that can be supported by this estimation approach is only around 100 for the frequency range $2\,\text{kHz} < \bar{f}_i < 4\,\text{kHz}$ and response time $T < 0.1$ s.

In many practical lighting applications, however, a significantly larger number of LEDs needs to be supported, e.g., [7], [9], and [10]. In this paper, therefore, we develop an estimation approach that yields superior performance in comparison to the estimator that uses only the fundamental frequency component. Specifically, we try to reduce the induced interference between different LED signals, as well as exploit more signal power from the sensor signal. To this end, we consider using higher order harmonics in this paper. This approach is attractive for two reasons. First, there is a larger frequency separation between the higher harmonics of two adjacent frequencies. For instance, the spacing is $m\Delta_f$ in the mth harmonic, i.e., m times the spacing in the fundamental frequency range. In the presence of frequency offsets, the spacing between the mth harmonic of two actual frequencies $mf_{i+1} - mf_i = m\Delta'_{f,i}$ is also m times of the spacing $f_{i+1} - f_i = \Delta'_{f,i}$. If the signals from different LEDs are disentangled based on the mth harmonic of the sensor signal for the purpose of estimating $\{a_i\}$, we only need to consider the spacing $m\Delta'_{f,i}$ and set $m\Delta_f$ to be sufficiently large, e.g., $m\Delta_f > 2/T$. Therefore, we can possibly achieve a much

smaller Δ_f if a higher order harmonic is exploited. Equivalently, a larger number of frequencies $\{f_i\}$ can potentially be packed in the given frequency range. Secondly, we can utilize the power in the higher order harmonics of the sensor signal. This is especially useful in the situation when the individual estimation performs worst, *viz.* when p_i is close to 0 or 1, in which case the bulk of the signal power lies in the higher order harmonics rather than the fundamental frequency component.

When multiple harmonics are considered, the signal from the ith LED consists of multiple sinusoids whose frequencies are multiples of the same fundamental frequency f_i. The objective of illumination sensing is then to estimate the parameters of these sinusoids. The problem of sinusoid parameter estimation has attracted a lot of research interest in literature. However, the literature focuses either on parameter estimation of multiple sinusoids that are not harmonically related, e.g., [11]–[14], or on parameter estimation using multiple harmonics for a single source, e.g., [15]. The problem in this paper, i.e., multiple harmonics from each of multiple sources, as such is fundamentally different from previous works. New challenges arise in this problem setting. One of the key questions concerns the performance limit with the use of multiple harmonics. More specifically, it is important to understand the limit on the number of LEDs that can be supported. Provided that there is indeed significant potential to support a large number of LEDs, another key challenge is then how to design an estimation approach with manageable computational complexity to materialize this potential. All these issues will be addressed in this paper.

In our previous work [16], we have introduced a successive estimation approach based on multiple harmonics. In this paper, we consider the approach in more detail. We derive upper limits on the number of LEDs that can be supported, based on Cramér–Rao bound (CRB) analysis. Further, the computation complexity of the algorithm is also provided along with more extensive simulations.

The rest of this paper is organized as follows. After a detailed problem description in Section II, upper limits on the number of LEDs that can be supported are derived in Section III. Thereafter, a low complexity successive estimation approach and an associated LED grouping and frequency allocation scheme are presented in Section IV. The computational complexity of the proposed approach is also analyzed. Simulation results to address the performance of the estimator are presented in Section V, vis-a-vis the upper limits presented in Section III. Finally, Section VI concludes this paper.

II. Problem Description

The sensor signal at the output of the photosensor is given by

$$y(t) = \sum_{i=1}^{L} y_i(t) + v(t) = \sum_{i=1}^{L} a_i \sum_{n=-\infty}^{\infty} \mathrm{rect}\Big(\frac{f_i(t+\theta_i)-n}{p_i}\Big) + v(t) \quad (2)$$

where L is the number of LEDs and is assumed to be known from system installation. The sensor signal component $y_i(t)$ is due to the ith LED, and $\mathrm{rect}(t)$ is a rectangular function with $\mathrm{rect}(t) = 1$ when $|t| \le 1/2$ and $\mathrm{rect}(t) = 0$ elsewhere. The value of p_i is prescribed by the central controller and also known to the sensor. Each $y_i(t)$ thus consists of a pulse train with an amplitude a_i, an initial phase θ_i and a frequency f_i. The amplitude a_i characterizes the illumination contribution of the ith LED, and is the primary parameter to be estimated. The phase θ_i is unknown since there is no synchronism between the spatially distributed LEDs and between the LEDs and the sensor. The frequency $f_i = \bar{f}_i + \epsilon_i$ is not exactly known due to the frequency offset ϵ_i, although the ideal frequency $\bar{f}_i$ is known as the identifier for the ith LED. Moreover, the frequency offset ϵ_i is considered to be within bounded values [17] and the fluctuation of the offset value is considered negligible within the considered response time such as $T = 0.1$ s. The bounded values are normally represented by the relative ratio η, in terms of parts per million (ppm), with respect to the actual frequency $\bar{f}_i$, i.e., $|\epsilon_i| \le \bar{f}_i \eta$.

The ideal frequency $\bar{f}_i$, as introduced in Section I, is allocated between $f_{\min} = 2$ kHz and $f_{\max} = 4$ kHz, i.e., the considered bandwidth is $W = f_{\max} - f_{\min} = 2$ kHz. In [7], the $\{\bar{f}_i\}$ are allocated uniformly between $f_{\min}$ and $f_{\max}$ with a frequency spacing Δ_f between adjacent frequencies. In this paper, however, as will be explained later, we divide the frequency range $(f_{\min},\ f_{\max})$ into M sub-ranges. The ideal frequencies $\{\bar{f}_i\}$ in each mth subrange are still uniformly allocated with a frequency spacing $\Delta_{f,m}$, except that $\Delta_{f,m}$ decreases as m increases. Nevertheless, the value of $\bar{f}_i$ is always known to the sensor as the identifier for the ith LED. The value of θ_i can be anywhere between $-1/(2f_i)$ and $1/(2f_i)$. To obtain an accurate estimate of a_i, the values of f_i and θ_i also need to be estimated. The noise term $v(t)$, consisting of electronic and shot noise, is assumed to be additive white Gaussian noise with double-sided power spectrum density $N_0/2$. For a practical indoor environment [7] with an illuminance of 1000 lux and a photodiode with an area of 10 mm^2, N_0 is in the order of 10^{-24} ampere^2/Hz. To estimate $\{a_i, f_i, \theta_i\}$, it is convenient to express $y_i(t)$ in the form of harmonics, i.e.,

$$y_i(t) = a_i \sum_{m=0}^{\infty} 2b_{i,m} \cos(2\pi m f_i t + m\phi_i), \quad (3)$$

where $b_{i,m}$ is the magnitude of the mth harmonic. Note that this paper deals with baseband signals from unsynchronized LEDs, and there is no in-phase and quadrature components analysis of the signals [14, Ch. 5.4]. Therefore, we focus on the real-valued cosine signal model in (3) instead of complex-valued exponential signal models. For a rectangular pulse with a known duty cycle p_i, we have a known $b_{i,m}$ given by $b_{i,m} = \sin(\pi m p_i)/(\pi m)$. Note that, under practical protocols for PWM light dimming control [18], we have $p_{\min} = 0.001 \le p_i \le p_{\max} = 0.973$. The phase term is $\phi_i = 2\pi f_i \theta_i$. The estimation of $\{a_i, f_i, \theta_i\}$ is then transformed to the estimation of $\{a_i, f_i, \phi_i\}$.

For the estimation of $\{a_i\}$, the key requirements concern speed and accuracy. The first requirement is that the response time $T \le 0.1$ s. The second requirement is that the estimation results should be accurate enough such that the estimation error

is *invisible* to human eyes. More specifically, as long as the cost function [7], [19]

$$\xi_i \triangleq 10\log_{10}\left(\frac{|\hat{a}_i - a_i|p_i}{\sum_{l=1}^{L} a_l p_l}\right) \leq -20\ (\mathrm{dB}) \tag{4}$$

where $\hat{a}_i$ denotes the estimated value for a_i, the estimation error is considered acceptable.

With the above requirements on speed and accuracy being satisfied, the key challenge is to design an estimator so as to accommodate more LEDs, compared to [7], by allowing a smaller spacing between adjacent frequencies. In [7], only the term $m = 1$ in (3) is used for the estimation of a_i. In contrast, we shall exploit multiple harmonics in this paper.

Further, in (3), the direct current (DC) components with $m = 0$ for different i are not distinguishable, and hence are of no use for the purpose of illumination sensing. The useful signal power lies in all the other harmonics. Given $T \gg 1/f_i$, the DC component equals $(1/T)\int_{t=0}^{T} y_i(t)\mathrm{d}t = a_i p_i$ for each ith LED. Hence, the useful signal power of the ith LED is

$$\begin{aligned} P_i &= \frac{1}{T}\int_{t=0}^{T}(y_i(t) - a_i p_i)^2 \mathrm{d}t \\ &= \frac{1}{T}\int_{t=0}^{T} y_i^2(t)\mathrm{d}t - a_i^2 p_i^2 = a_i^2 p_i(1-p_i). \end{aligned} \tag{5}$$

Considering a noise bandwidth to be proportional to W, we define the signal-to-noise ratio as

$$\zeta_i = 10\log_{10}\frac{P_i}{N_0 W} = 10\log_{10}\frac{a_i^2 p_i(1-p_i)}{N_0 W}\ (\mathrm{dB}). \tag{6}$$

The maximum value of a_i, e.g., when a sensor lies in the center of a narrow LED beam, is in the order of 10^{-6} ampere. For each i, the worst case SNR occurs when $p_i = p_{\min}$. Hence, from (6), we can get, for $T = 0.1$ s, that

$$\max_i(\zeta_i) = 57\ (\mathrm{dB}). \tag{7}$$

III. Performance Limits

In this section, before applying any specific algorithms, we investigate the potential parameter estimation performance that can be obtained by exploiting multiple harmonics. Specifically, there are two limiting factors. One is due to the influence of frequency offsets on the ability to identify different LEDs. The other concerns the influence of noise and is based on the study of the Cramér–Rao bound (CRB).

A. Number of Distinguishable LEDs in the Presence of Frequency Offset

In the FDM scheme, we use frequencies as the identifiers of the LEDs. The frequencies are thus allocated in a strict order, i.e., $\bar{f}_i < \bar{f}_{i+1}$. If, due to the frequency offsets, the order of the actual frequencies is changed, e.g., $f_i > f_{i+1}$ for some i, the sensor will not be able to identify these two LEDs correctly. Hence, the spacing between allocated frequencies should be large enough to avoid this issue. Assuming the relative clock accuracy is denoted by η, i.e., the frequency offset $|\epsilon_i| \leq \bar{f}_i\eta$, as introduced in Section II, we get that the actual spacing between two adjacent frequencies is $\Delta'_{f,i} = f_{i+1} - f_i = \bar{f}_{i+1} - \bar{f}_i + \epsilon_{i+1} - \epsilon_i$. The minimum value of $\Delta'_{f,i}$ is thus $\min(\Delta'_{f,i}) = \bar{f}_{i+1} - \bar{f}_i - (\bar{f}_i + \bar{f}_{i+1})\eta$. In order to maintain $\Delta'_{f,i} \geq 0$, we should have $\min(\Delta'_{f,i}) \geq 0$, hence

$$\bar{f}_{i+1} \geq r\bar{f}_i \tag{8}$$

where

$$r \triangleq \frac{1+\eta}{1-\eta}. \tag{9}$$

By induction, we get that $\bar{f}_L \geq r^{L-1}\bar{f}_1$. Given that $f_{\max} \geq \bar{f}_i \geq f_{\min}$ for any i, we further have

$$f_{\max} \geq \bar{f}_L \geq r^{L-1}\bar{f}_1 \geq r^{L-1} f_{\min}. \tag{10}$$

Thus, we get

$$L \leq \frac{\ln\left(\frac{f_{\max}}{f_{\min}}\right)}{\ln r} + 1. \tag{11}$$

Note that, in order to achieve this upper limit, the ideal frequencies $\{\bar{f}_i\}$ should be assigned in an exponential scale, i.e., $\bar{f}_i = f_1 r^{i-1}$.

For a low cost design, the clock inaccuracy is assumed to be $\eta = 100$ ppm $= 10^{-4}$. From (11) and $f_{\max} = 2f_{\min}$, this implies $L \leq 3466$.

B. Limit on the Estimation Accuracy

Here, we consider the effect of noise on the estimation performance based on the Cramér–Rao bound (CRB), which gives a lower bound on the variance of the estimation error for any unbiased estimator. In fact the CRB can be approximately achieved by a maximum likelihood (ML) estimator at high SNR [12]. Thus, in this paper, we consider the CRB as an indicator of the maximum achievable performance. Of particular interest in this paper is the maximum number of LEDs that can be supported when the estimation error is bounded. Equivalently, given the limited bandwidth to assign the frequencies $\bar{f}_i$, we investigate the CRB at different Δ_f between adjacent frequencies.

For illumination sensing, the estimation performance is measured in terms of $\{\hat{a}_i\}$, see (4). We therefore focus on the accuracy in amplitude estimation when the frequencies $\{f_i\}$ and phases $\{\phi_i\}$ are unknown, as explained in Section II. Let σ_i^2 denote the CRB on the estimation of a_i. The smallest MSE achievable by an ML estimator is $\mathbb{E}\{(\hat{a}_i^{\mathrm{ML}} - a_i)^2\} = \sigma_i^2$, where $\mathbb{E}\{\cdot\}$ denotes the expectation operation and $\hat{a}_i^{\mathrm{ML}}$ is the estimated value by an ML estimator. In the ML estimator, a_i is fixed, while $\hat{a}_i^{\mathrm{ML}}$ is random due to the presence of random noise $v(t)$ in $y(t)$. Therefore, the expectation is taken over all realizations of $\hat{a}_i^{\mathrm{ML}}$.

Based on the definition (4), we consider the following cost function:

$$\hat{\xi}_i \triangleq 10\log_{10}\left(\frac{\sigma_i p_i}{\sum_{l=1}^{L} a_l p_l}\right). \tag{12}$$

It can be shown that $\hat{\xi}_i$ represents the worst case for the expected performance of the ML estimator, i.e.,

$$\mathbb{E}\{\xi_i^{\mathrm{ML}}\} \le \hat{\xi}_i, \tag{13}$$

where ξ_i^{ML} is defined, according to (4), as

$$\xi_i^{\mathrm{ML}} \triangleq 10\log_{10}\left(\frac{|\hat{a}_i^{\mathrm{ML}} - a_i| p_i}{\sum_{l=1}^{L} a_l p_l}\right). \tag{14}$$

Proof: To prove (13), consider that

$$\begin{aligned}\mathbb{E}\left\{\log|\hat{a}_i^{\mathrm{ML}} - a_i|\right\} &= \frac{1}{2}\mathbb{E}\left\{2\log\left(|\hat{a}_i^{\mathrm{ML}} - a_i|\right)\right\} \\ &= \frac{1}{2}\mathbb{E}\left\{\log\left((\hat{a}_i^{\mathrm{ML}} - a_i)^2\right)\right\}. \end{aligned}\tag{15}$$

Due to Jensen's inequality [20, chap 3.14] and since the function $\log(\cdot)$ is a concave function, we have

$$\begin{aligned}\mathbb{E}\left\{\log\left((\hat{a}_i^{\mathrm{ML}} - a_i)^2\right)\right\} &\le \log(\mathbb{E}\{(\hat{a}_i^{\mathrm{ML}} - a_i)^2\}) \\ &= \log\sigma_i^2. \end{aligned}\tag{16}$$

From (15) and (16), we have $\mathbb{E}\left\{\log|\hat{a}_i^{\mathrm{ML}} - a_i|\right\} \le \log\sigma_i$. Then based on (12) and (14), we have

$$\begin{aligned}\mathbb{E}\{\xi_i^{\mathrm{ML}}\} &= 10\,\mathbb{E}\{\log_{10}(|\hat{a}_i^{\mathrm{ML}} - a_i|)\} - 10\log_{10}\left(\frac{p_i}{\sum_{l=1}^{L} a_l p_l}\right) \\ &\le 10\log_{10}\sigma_i - 10\log_{10}\left(\frac{p_i}{\sum_{l=1}^{L} a_l p_l}\right) = \hat{\xi}_i. \end{aligned}$$

■

From (13), $\hat{\xi}_i$ represents the worst case performance of the optimum ML estimator. We will then use $\hat{\xi}_i$ as a reference to investigate the potential estimation performances. From (4), we additionally require that $\hat{\xi}_i \le -20$ (dB).

In order to obtain $\hat{\xi}_i$, we first need to obtain the CRB σ_i^2. To this end, we let $\mathbf{u}$ denote the vector of unknown parameters, i.e., $\mathbf{u} \triangleq [a_1, a_2, \ldots, a_L, \phi_1, \phi_2, \ldots, \phi_L, f_1, f_2, \ldots, f_L]^T$, where $[\cdot]^T$ denotes the operation of matrix transpose. We can then obtain the Fisher information matrix $\mathbf{J}$ of size $3L \times 3L$. The (m,n)th element of $\mathbf{J}$ equals

$$J_{m,n} = \frac{2}{N_0}\mathbb{E}\left(\int_{t=0}^{T} \frac{\partial y(t)}{\partial u_m}\frac{\partial y(t)}{\partial u_n}\mathrm{d}t\right), \tag{17}$$

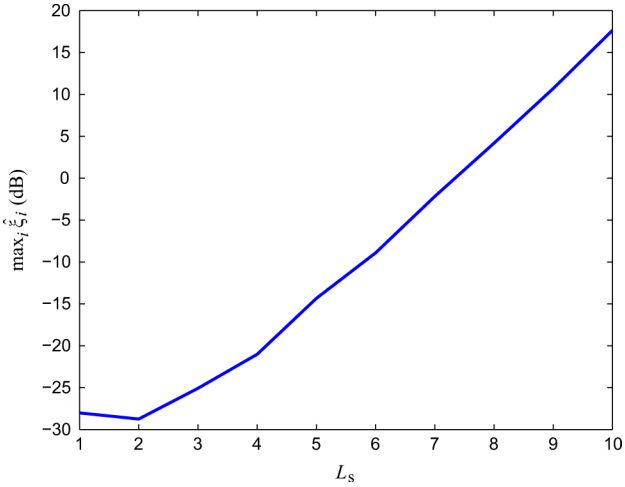

Fig. 3. Estimation performance bound for different number of LEDs, when $\Delta_f = 10$ Hz and only the fundamental frequency component is considered, $T = 0.1$ s, $\phi_i = 0$, $p_i = p_{\min}$, $f_i = f_{\min} + (i-1)\Delta_f$, SNR $\zeta_i = 57$ dB, for $i = 1$ to L_s, and $a_i = a_k$ for $i \ne k$.

where u_m and u_n denote the mth and nth element of the vector $\mathbf{u}$, respectively. The CRB on the estimation error of the parameter a_i for $i = 1$ to L can be obtained [11] as $\sigma_i^2 = [\mathbf{J}^{-1}]_{i,i}$, i.e., the ith diagonal element of the matrix $\mathbf{J}^{-1}$. In the following, we first discuss the CRBs when there is no frequency offsets and later analyze the the impact of frequency offsets.

1) No Frequency Offsets: For convenience of investigation, we first ignore the frequency offsets when discussing the CRB. In this case, the CRB is mainly determined by the noise level and the spacing Δ_f. Of particular interest is the minimum Δ_f that yields adequate estimation performance. Moreover, in order to allocate as many LEDs as possible, we assume a uniform frequency spacing between the LEDs, where every spacing is equal to the obtained minimum spacing.

Fundamental Frequency Component: When only the fundamental frequency components are considered, the parameter estimation of multiple pulse trains studied in this paper is equivalent to the parameter estimation of multiple sinusoids. The CRB for this problem has been computed in [11], [12]. It was shown that the characteristics of the CRB are dependent on the frequency spacing, denoted by Δ_f, between different sinusoids. Specifically, there is a threshold, denoted by $\Gamma_1 \approx 1/T$, on Δ_f [11]. If $\Delta_f > \Gamma_1$, the CRB in the presence of multiple sinusoids appears to be close to that when there is only a single sinusoid. This CRB is thus also named asymptotic CRB in [12]. On the other hand, if $\Delta_f \le \Gamma_1$, the CRB increases rapidly with the number of sinusoids. Moreover, the values of the non-asymptotic CRB are highly dependent on the actual values of $\{a_i, f_i, \phi_i\}$.

In this paper, given a response time $T \le 0.1$ s, and the target to support much more than 100 LEDs as achieved in [7], we need to consider the non-asymptotic CRB. Moreover, in contrast to [11] where numerical results for more than three sinusoids were not presented, we consider $L \gg 3$. By way of example, we consider the case $p_i = p_{\min}$, $f_i = 2000 + (i-1)\Delta_f$, and

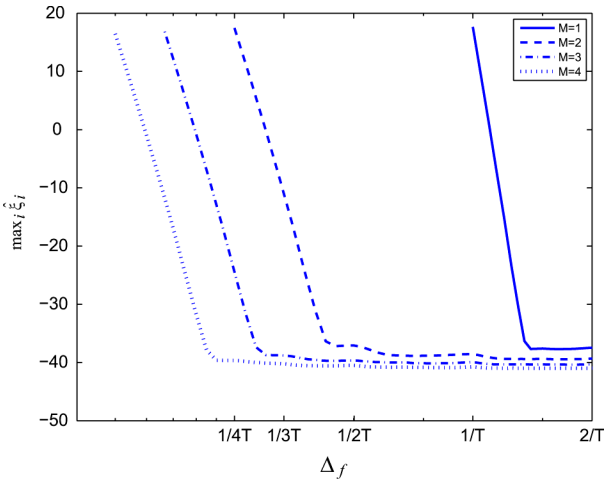

Fig. 4. Estimation performance bound at different frequency spacing when up to M harmonics are considered, $L_{\rm s}=10$, $T=0.1$ s, $\phi_i=0$, $p_i=p_{\min}$, $f_i=f_{\min}+(i-1)\Delta_f$, SNR $\zeta_i=57$ dB, for $i=1$ to $L_{\rm s}$, and $a_i=a_k$ for $i\neq k$.

$\phi_i=0$ for every i, and $a_i=a_k$ for $i\neq k$. In this duty cycle setting, the power in the fundamental frequency component is minimal, and thus this is a difficult case for the estimator when only the fundamental frequency components are considered. Further, as the induced interference is one of the most important performance limiting factors, we consider the case when all the LEDs have the same illuminances such that there are equally strong interferences between the LEDs with neighboring frequencies. In practical simulations, we also consider the case when $a_i\neq a_k$, as will be discussed in Section V. Moreover, we consider $\Delta_f=10$ Hz here to support at least 200 LEDs. Then, we consider the scenarios when only the LEDs with $i=1$ to $L_{\rm s}$ are switched on. With $L_{\rm s}$ increasing from 1 to 10, we can obtain the value of worst case performance among all the LEDs, i.e., $\max_i\{\hat{\xi}_i\}$, as presented in Fig. 3. It can be seen that the estimation bound increases significantly when $L_{\rm s}$ increases beyond 3, and the requirement $\hat{\xi}_i\leq -20$ dB for all i cannot be satisfied. In other words, we cannot allow $\Delta_f\leq 10$ Hz if only the fundamental frequency component is used.

Note that, when $L_{\rm s}=1$, the CRB is determined only by noise and we can obtain from [21] that

$$\sigma_1^2=\frac{N_0}{4b_{1,1}^2T}, \tag{18}$$

where $b_{1,1}$ characterizes the amplitude of the fundamental frequency component, as in (3), and $b_{1,1}=\sin(\pi p_1)/\pi$. Hence we have that

$$\begin{aligned}\hat{\xi}_1&=10\log_{10}\frac{\sigma_1 p_1}{a_1p_1}=10\log_{10}\sqrt{\frac{N_0}{4a_1^2b_{1,1}^2T}}\\&=-\frac{1}{2}\zeta_i+5\log_{10}\frac{p_1(1-p_1)}{4b_{1,1}^2}.\end{aligned} \tag{19}$$

When $T=0.1$ s and $\zeta_1=57$ dB, we have $\hat{\xi}_1=-28$ dB, as can be seen in Fig. 3. When $L_{\rm s}>1$, however, there is no analytical form for σ_1^2. Further, the value $\max_i\hat{\xi}_i$ slightly decreases when $L_{\rm s}$ increases from 1 to 2, although there is an increase in σ_i. The reason is that there is a normalization factor $\sum_{l=1}^{L_{\rm s}}a_lp_l$ for σ_i due to the definition of the cost function in (12). When $L_{\rm s}$ increases from 1 to 2, the increase in σ_i is overshadowed by the increase of the normalization factor. When $L_{\rm s}$ increases beyond 2, the speed of increase in σ_i is much faster than the increase in the normalization factor. The value $\max_i\hat{\xi}_i$ hence keeps increasing with $L_{\rm s}>2$.

Multiple Harmonics: Now, we consider using higher order-harmonics besides the fundamental frequencies. From numerical results, as illustrated in Fig. 4, we can conclude that there is also a threshold on the frequency separation, $\Gamma_M\approx 1/(MT)$, when up to M harmonics are considered. When $\Delta_f\leq\Gamma_M$, the CRB increases dramatically with the decrease of Δ_f, and consequently, the requirement $\hat{\xi}_i<-20$ dB for every i can not be satisfied.

When $\Delta_f>\Gamma_M$, the asymptotic CRB applies. Thus we have [15]

$$\sigma_i^2=\frac{N_0}{4T\sum_{k=1}^{M}b_{i,k}^2}. \tag{20}$$

For the case $p_i=p_{\min}$ for every i and $a_i=a_k$ for $i\neq k$, we have

$$\begin{aligned}\hat{\xi}_i&=10\log_{10}\frac{\sigma_i p_i}{\sum_{l=1}^{L_{\rm s}}a_lp_l}=10\log_{10}\frac{\sigma_i}{L_{\rm s}a_i}\\&=-\frac{1}{2}\zeta_i+5\log_{10}\frac{p_1(1-p_1)}{4L_{\rm s}^2\sum_{k=1}^{M}b_{i,k}^2}\end{aligned} \tag{21}$$

as numerically shown in Fig. 4, for $L_{\rm s}=10$, $T=0.1$ s and $\zeta_i=57$ dB.

Thus, the maximum number of LEDs that can be supported can be written as

$$L_M=\frac{W}{\Gamma_M}\approx MTW=200M. \tag{22}$$

Clearly, L_M is linearly proportional to M. This indicates the potential of supporting more LEDs with the use of higher harmonics. Note that the basis of this linear relationship is that the Mth harmonic is strong enough to be utilized for the separation of the signals from different LEDs. When M becomes larger, however, the strength of the Mth harmonics, which is approximately proportional to $1/M$, tends to be weaker. The linear relation in (22) will thus not hold for an extremely large M. In particular, when $M\to\infty$, L_M converges to a fixed value, denoted by L_∞, as will be discussed next.

Infinite Number of Harmonics: When $M\to\infty$, the shape of the pulse trains become exactly rectangular. The CRB can be obtained correspondingly. Similar to the analysis on CRB when $M<\infty$, we are particularly interested in the threshold Γ_∞ with respect to Δ_f such that the square pulse trains can be viewed as uncorrelated if $\Delta_f>\Gamma_\infty$. To obtain Γ_∞, we consider two rectangular pulse trains with close frequencies. Further, it is most difficult to distinguish the two pulse trains if they have identical duty cycles. Hence we focus on the case when both duty cycles are equal to $p_{\min}$, as it is the most interesting case to study the estimation performance with the use of the multiple

harmonics. Heuristically, if such two pulse trains keep overlapping each other within the response time T, it is difficult to distinguish them. Given the fact that there is always a relative shift between such pulse trains due to the frequency difference Δ_f, Γ_∞ can be approximated obtained by the following procedure.

Given two frequencies f_1 and $f_2 = f_1 + \Delta_f$. In every $1/f_1$ interval, there is a relative shift of $\Delta_f/(f_1 f_2)$ between these two pulse trains. Within the response time T, there is a relative shift

$$\frac{T}{\frac{1}{f_1}} \cdot \frac{\Delta_f}{f_1 f_2} = \frac{T\Delta_f}{f_2}. \tag{23}$$

The threshold Γ_∞ can be determined such that the relative shift when $\Delta_f = \Gamma_\infty$ is as large as the width of a single pulse $p_{\min}/f_2$, i.e., $T\Gamma_\infty/f_2 = p_{\min}/f_2$. Hence, we get

$$\Gamma_\infty = \frac{p_{\min}}{T} \tag{24}$$

$$L_\infty = \frac{W}{\Gamma_\infty} = \frac{WT}{p_{\min}}. \tag{25}$$

For the case $T = 0.1$ s, we have $L_\infty = 2 \times 10^5$.

Since $L_\infty \gg L_M$, see (22), for the range of M that is of practical interest to this paper, we only consider the relation (22), unless specified otherwise. The discussion on the transient behavior of L_M between (22) and the convergence value shown above is beyond the interest of this paper.

To summarize, in the absence of frequency offsets, we obtained that the number of LEDs that can be potentially supported is linearly proportional to the number of harmonics that are used, up to a limit that is determined by L_∞.

2) Impact of Frequency Offsets: In the presence of frequency offsets, the real frequency spacing $\Delta'_{f,i} = f_{i+1} - f_i$ is unequal to $\Delta_f = \bar{f}_{i+1} - \bar{f}_i$. We thus should make sure that $f_{i+1} - f_i$ is larger than the threshold Γ_M for different M. As discussed in Section III-A, the minimum value of $\Delta'_{f,i}$ is $\min(\Delta'_{f,i}) = \bar{f}_{i+1} - \bar{f}_i - (\bar{f}_i + \bar{f}_{i+1})\eta$. From $\min(\Delta'_{f,i}) \geq \Gamma_M = 1/(MT)$, we can obtain

$$\bar{f}_{i+1} \geq r\bar{f}_i + c \tag{26}$$

where r is defined in (9) and

$$c \triangleq \frac{1}{(MT(1-\eta))}. \tag{27}$$

By induction, we have

$$\begin{aligned} f_{\max} \geq f_L &\geq r^{L-1}\bar{f}_1 + c\frac{r^{L-1}-1}{r-1} \\ &\geq r^{L-1}\bar{f}_{\min} + c\frac{r^{L-1}-1}{r-1}. \end{aligned} \tag{28}$$

Thus, we get

$$L \leq \frac{\ln \frac{(r-1)f_{\max}+c}{(r-1)f_{\min}+c}}{\ln r} + 1. \tag{29}$$

Substituting (9) and (27) into (29), we get

$$L \leq \frac{\ln \frac{f_{\max}+\frac{1}{MT\eta}}{f_{\min}+\frac{1}{MT\eta}}}{\ln r} + 1. \tag{30}$$

When $M \to \infty$, we get $c \to 0$ and that the bound in (30) converges to that in (11). Note that, from the discussion on the case of infinite harmonics in Section III-B-I, we should in fact consider Γ_∞ in (24) to obtain a tighter bound for the case $M \to \infty$. Similar to the derivation of (30), we can obtain the bound

$$L \leq \frac{\ln \frac{f_{\max}+\frac{p_{\min}}{T\eta}}{f_{\min}+\frac{p_{\min}}{T\eta}}}{\ln r} + 1. \tag{31}$$

In a practical situation with $T = 0.1$ s and $\eta = 100$ ppm, the bounds in (30) and (31) are equal to 3466 and 3346, respectively. Hence, there is only a minor difference between these two bounds as $M \to \infty$. In the following numerical results, we thus only consider (30) for convenience.

In Fig. 5(a), we show the number of LEDs that can potentially be supported at different response time T with the clock inaccuracy $\eta = 100$ ppm. At a larger T, a larger number, L, of LEDs can be supported with the same number, M, of harmonics when $M < \infty$. However, when $M \to \infty$, there is a common upper limit prescribed by η, see (11), for every T. Moreover, when T is fixed and η changes, the numerical results are shown in Fig. 5(b). When M is small, the number of LEDs that can be supported is mainly determined by T, and hence the difference due to different η is not significant. However, when $M \to \infty$, there is a much larger potential on L for a smaller η. Finally, as shown in Fig. 5, at the typical condition $T = 0.1$ s and $\eta = 100$ ppm, we can increase the number of LEDs by an order of magnitude through exploiting multiple harmonics of the sensor signal.

IV. Successive Estimator

To exploit the high performance potential through the use of multiple harmonics as discussed in Section III, in this section, we propose a practical estimator that utilizes multiple harmonics.

A. Frequency Domain Perspective

We describe the proposed estimator from a frequency domain perspective. Due to the required limited response time T, we are limited to use only the sensor signal in a T interval. Equivalently, the sensor signal $y(t)$ is multiplied with a windowing function $g(t)$ with a time span T. In the Fourier domain, we have

$$\begin{aligned} Y(f) &= \mathcal{F}[y(t)g(t)] \\ &= \sum_{i=1}^{L} \mathcal{F}[y_i(t)g(t)] + \mathcal{F}[v(t)g(t)] \\ &= \sum_{i=1}^{L} Y_i(f) + V(f) \end{aligned} \tag{32}$$

where

$$\begin{aligned} Y_i(f) &= \sum_{m=-\infty}^{\infty} Y_{i,m}(f) \\ &= \sum_{m=-\infty}^{\infty} a_i b_{i,m} e^{jm\phi_i} G(f - mf_i). \end{aligned} \tag{33}$$

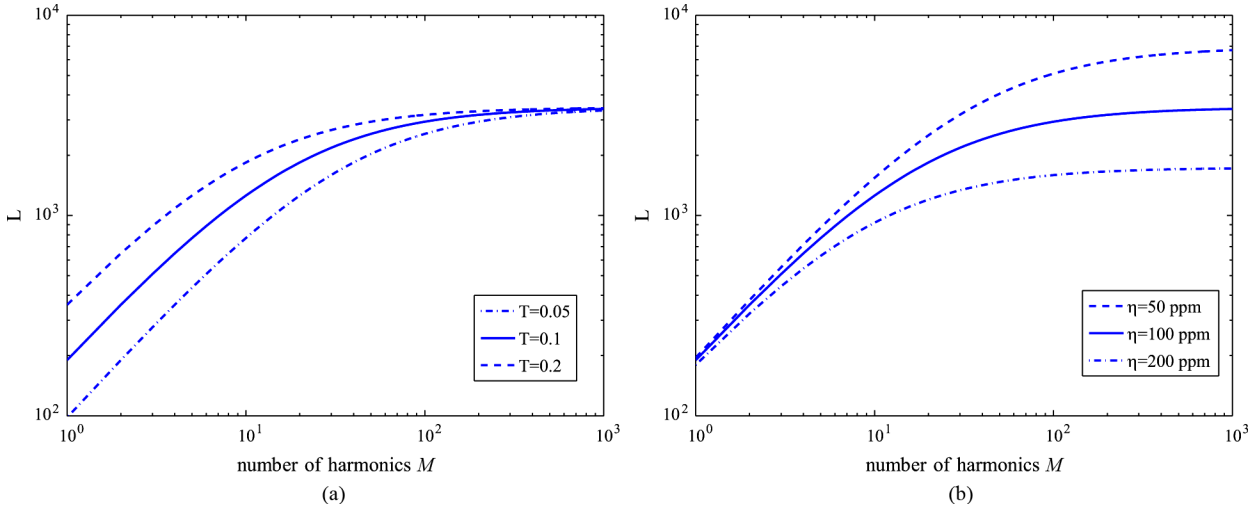

Fig. 5. Number of LEDs that can be supported when M harmonics are considered, $W = 2$ kHz (a) $\eta = 100$ ppm, at different T (b) $T = 0.1$ s, at different η.

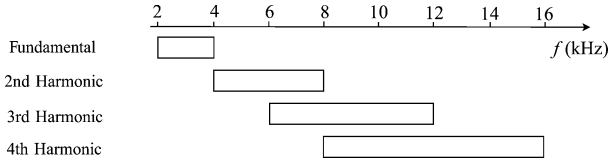

Fig. 6. Frequency range for different harmonics.

Here, $Y_i(f)$ is the Fourier transform of the windowed signal from the ith LED $Y_i(f) = \int_{-\infty}^{\infty} y_i(t)g(t)e^{-j2\pi ft}\mathrm{d}t$, $Y_{i,m}(f)$ denotes the mth harmonic component in $Y_i(f)$ and $G(f)$ is the Fourier transform of $g(t)$. Without loss of generality, we let $G(0) = 1$. The Fourier transform of the windowed noise term is denoted by $V(f)$.

In order to utilize multiple harmonics for the estimation of $\{a_i, f_i, \phi_i\}$, we first look at the frequency ranges for different m, as illustrated in Fig. 6, for $m = 1$ to 4. It can be seen that the frequency ranges for different m overlap each other. This overlap indicates that there is mutual interference between different harmonics from different LEDs, and the interference is dependent on the phases $\{\phi_i\}$ that are unknown. Hence, it is not straightforward to use the mth harmonic and support m times more LEDs.

B. Successive Estimation Procedure

A closer inspection of Fig. 6 indicates that there is no frequency overlap in the frequency range between 4 kHz to 6 kHz in the second harmonic range. Hence, there is no interference from other harmonics. An estimator can thus be built based on this second harmonic frequency range to obtain estimates, $\{\hat{a}_i, \hat{f}_i, \hat{\phi}_i\}$, for the LEDs with $4\text{ kHz} < 2f_i < 6$ kHz. We call this estimator the *Component Estimator*, as it is a component of the successive estimation process described later in this section.

Before describing such component estimators in further detail, we extend the results from [7] on the spacing between two fundamental frequencies into the case of higher harmonics and obtain the following frequency spacing criterion: *When the* mth *harmonic frequency component is used, as long as the frequency spacing between two adjacent* mth *order harmonics, i.e.,* $m\bar{f}_{i+1} - m\bar{f}_i = m\Delta_f$, *satisfies* $m\Delta_f \geq 2/T$, *the estimates* $\{\hat{a}_i, \hat{f}_i, \hat{\phi}_i\}$ *are sufficiently accurate in the sense of* (4), *with response time* T. The above criterion applies when there is no interference from other harmonics and when the triangular windowing function [7] is applied. Since we have $\Delta_f = 2/(mT)$, the frequencies $\{f_i\}$ can be more closely packed by a factor of m, in comparison to that in [7]. A larger number of LEDs can thus be supported using higher order harmonics while maintaining adequate estimation performance. Due to the frequency overlap as illustrated in Fig. 6, it is, however, not possible to estimate every $\{\hat{a}_i, \hat{f}_i, \hat{\phi}_i\}$ using the highest possible harmonic order. Instead, in this paper, we propose a grouping strategy and a successive estimation procedure.

In the grouping strategy, the LEDs are divided into M groups. Correspondingly, the fundamental frequency range between $f_{\min}$ and $f_{\max}$ is also divided into M non-overlapping regions. We have a uniform frequency allocation within each mth group with a frequency spacing denoted by $\Delta_{f,m}$, where $m = 1$ to M. The value of $\Delta_{f,m}$, however, can be different for different m. Based on the grouping strategy, we propose a successive estimation procedure to obtain $\{\hat{a}_i, \hat{f}_i, \hat{\phi}_i\}$. To elucidate the grouping strategy and the successive procedure, we first consider the case of $M = 2$ groups and then extend into a larger M.

1) Successive Procedure for $M = 2$*:* When $M = 2$, we consider the frequency range up to the second harmonic range, i.e., up to $2f_{\max} = 8$ kHz.

First, let us only consider the second harmonic range from $f_{\max}$ to $(4/3)f_{\max}$. Denote by *Group 1* all the LEDs with a second harmonic in this frequency range, or equivalently $(1/2)f_{\max} < f_i < (2/3)f_{\max}$. The frequency ranges of different harmonics corresponding to Group 1 are illustrated in Fig. 7 by the dark blocks. There is no frequency overlap between this second harmonic range of Group 1 and any other harmonic frequency range of any LEDs. The above spacing criterion thus applies here based on the second harmonics. Therefore, we have $\Delta_{f,1} = (2/T)/2$. Further denote the fundamental frequency range of Group 1 by W_1. Clearly, $W_1 = (4f_{\max}/3 - f_{\max})/2 = W/3$.

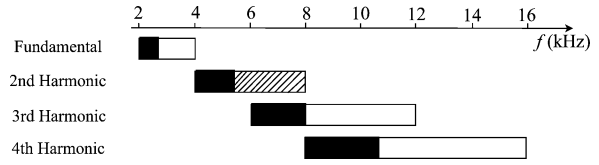

Fig. 7. Illustration of the successive estimator for $M = 2$. The dark regions correspond to the frequency ranges of the LEDs in Group 1. The shaded region illustrates the second harmonic range of the LEDs in Group 2.

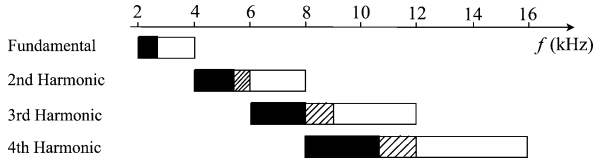

Fig. 8. Illustration of the successive estimator for $M > 2$. The dark and shaded regions correspond to the frequency ranges of the LEDs in Group 1 and 2, respectively.

Hence, the number of LEDs in Group 1, denoted by L_1, is $L_1 = 2W_1/(2/T) = WT/3$.

After estimating $\{\hat{a}_i, \hat{f}_i, \hat{\phi}_i\}$, for $i = 1$ to L_1, based on $\sum_{i=1}^{L_1} Y_{i,2}(f)$, we can also reconstruct $Y_{i,m}(f)$ for different m by

$$Y_{i,m}(f) \approx \hat{a}_i b_{i,m} e^{jm\hat{\phi}_i} G(f - m\hat{f}_i). \tag{34}$$

Then if we subtract all the components in $Y(f)$ that are due to the LEDs in Group 1, by

$$Y(f) - \sum_{m=0}^{\infty} \sum_{i=1}^{L_1} Y_{i,m}(f), \tag{35}$$

the overlap between the second and third harmonic ranges is removed, as seen from Fig. 7. Hence, using the component estimator in Section IV-C, we can estimate the parameters for the rest of the LEDs, named *Group 2*, based on their second harmonics, too. The second harmonic range for Group 2 is illustrated as the shaded blocks in Fig. 7. We can thus get $W_2 = (2/3)W$, and $L_2 = 2W_2/(2/T) = W_2T$. In this way, we can achieve $L = L_1 + L_2 = WT$ LEDs, which is twice as large as that in [7].

2) Successive Procedure for $M > 2$: The above grouping and successive estimation procedure for two groups can be generalized to the case of $M > 2$ groups. When $M > 2$, the frequency allocation for Group 1 remains the same as for $M = 2$, however the frequency allocation for Group 2 is changed, as illustrated in Fig. 8.

Here, the parameters $\{\hat{a}_i, \hat{f}_i, \hat{\phi}_i\}$ of the LEDs in Group 2 are estimated based on the third harmonics from $2f_{\max}$ to $(9/4)f_{\max}$. As can be seen in Fig. 8, this frequency region is overlap free in

$$Y(f) - \sum_{m=0}^{\infty} \sum_{i=1}^{L_1} Y_{i,m}(f), \tag{36}$$

i.e., after the frequency components of the Group 1, corresponding to the dark blocks in Fig. 8, are removed from $Y(f)$. Hence, the spacing criterion presented above applies here and we need to have $\Delta_{f,2} = (2/T)/3$ to obtain sufficiently accurate estimates $\{\hat{a}_i, \hat{f}_i, \hat{\phi}_i\}$ for the LEDs in Group 2. We thus obtain $W_2 = ((9/4)f_{\max} - 2f_{\max})/3 = W/6$ and $L_2 = W_2/\Delta_{f,2} = WT/4$.

Note that the upper limit $9/4f_{\max}$ of this third harmonic range is determined based on the following criterion: *After* $\sum_m \sum_{i=1}^{L_1+L_2} Y_{i,m}$, *i.e., the Fourier transform of the signals from both Group 1 and Group 2, is subtracted from* $Y(f)$, *the overlap between the fourth and third harmonic range is completely removed*. As such, if $M = 3$ the entire third frequency range is available to be used for the parameter estimation of the LEDs in the third groups. Alternatively, when $M > 3$, part of the fourth harmonic range starting from $3f_{\max}$ can be used for Group 3.

The above criterion can be further extended to other groups. By way of illustration, we consider Group $m-1$. In this group, the LEDs indices are $i = \mathcal{L}_{m-2} + 1$ to $\mathcal{L}_{m-1}$, where $\mathcal{L}_m = \sum_{k=1}^{m} L_k$. Based on the estimated results $\{\hat{a}_i, \hat{f}_i, \hat{\phi}_i\}$ for $i = 1$ to $\mathcal{L}_{m-2}$, i.e., the LEDs in the first $m-2$ groups, we can subtract the frequency components due to these LEDs by

$$\mathcal{Y}_m(f) = Y(f) - \sum_{i=1}^{\mathcal{L}_{m-2}} \hat{Y}_i(f). \tag{37}$$

where $\hat{Y}_i(f)$ is the estimated value of $Y_i(f)$, i.e.

$$\begin{aligned} \hat{Y}_i(f) &= \sum_{k=0}^{\infty} \hat{Y}_{i,k} \\ &= \sum_{k=0}^{\infty} \hat{a}_i b_{i,k} G(f - k\hat{f}_i) \exp(jk\hat{\phi}_i). \end{aligned} \tag{38}$$

Moreover, we focus on the mth harmonic frequency range for the $(m-1)$th group, from $(m-1)f_{\max}$ and $m^2 f_{\max}/(m+1)$. After the subtraction in (37), this becomes an overlap-free frequency range. Hence, we only need to consider

$$\begin{aligned} \mathcal{Y}_m(f) &\approx \sum_{i=\mathcal{L}_{m-2}+1}^{\mathcal{L}_{m-1}} Y_{i,m}(f) \\ &= \sum_{i=\mathcal{L}_{m-2}+1}^{\mathcal{L}_{m-1}} a_i b_{i,m} e^{jm\phi_i} G(f - mf_i). \end{aligned} \tag{39}$$

In order to obtain (39), the value of $\hat{Y}_i(f)$ should be accurate enough so that, in $\mathcal{Y}_m(f)$, there is ideally no frequency component due to the LEDs with $1 \le i \le \mathcal{L}_{m-2}$. However, there is always a residual error $Y_i(f) - \hat{Y}_i(f)$ in $\mathcal{Y}_m(f)$ due to the estimation error in $\{\hat{a}_i, \hat{f}_i, \hat{\phi}_i\}$ for $1 \le i \le \mathcal{L}_{m-2}$. This residual error will in turn result in larger errors in the estimates $\{\hat{a}_i, \hat{f}_i, \hat{\phi}_i\}$ for $\mathcal{L}_{m-2}+1 \le i \le \mathcal{L}_{m-1}$. This effect is referred to as error propagation. In order to limit the effect of error propagation, it is desirable to obtain a high accuracy in the estimation of $\{\hat{a}_i, \hat{f}_i, \hat{\phi}_i\}$ by the component estimator, as will be discussed in Section IV-C.

For the $(m-1)$th group, we take the mth harmonic range from $(m-1)f_{\max}$ to $m^2 f_{\max}/(m+1)$. Thus, we have $W_{m-1} = (m^2 f_{\max}/m - (m-1)f_{\max})/m = 2W/(m(m+1))$, since $W = f_{\max} - f_{\min} = f_{\max}/2$. The parameters of the LEDs are

TABLE I
PARAMETERS FOR THE DIFFERENT GROUPS FOR THE NEW ALLOCATION SCHEME

group	W_m/W	harmonic used	$\Delta_{f,m}$	L_m
1	1/3	2nd	$\frac{1}{T}$	$\frac{1}{3}WT$
$m < M$	$\frac{2}{(m+1)(m+2)}$	$(m+1)$th	$\frac{2}{(m+1)T}$	$\frac{1}{m+2}WT$
M	$\frac{2}{M+1}$	Mth	$\frac{2}{MT}$	$\frac{M}{M+1}WT$

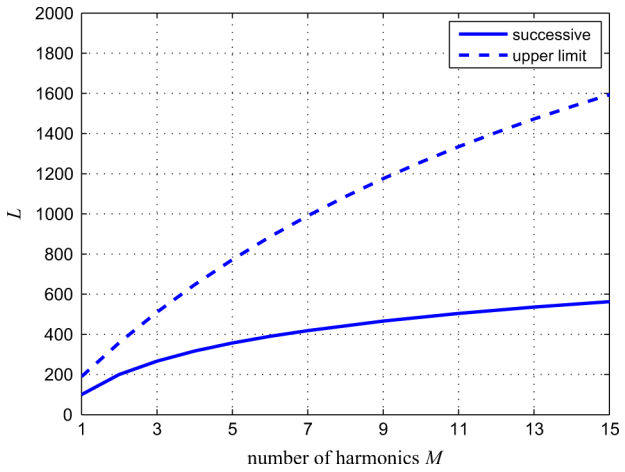

Fig. 9. Number of LEDs that can be supported by the successive estimation approach according to (40), compared to the upper limit according to (30), at $\eta = 100$ ppm and $T = 0.1$ s.

estimated based only on the mth harmonic signal. Hence, the equivalent frequency spacing between two adjacent frequencies in terms of $\{\bar{f}_i\}$ is $\Delta_{f,m-1} = 2/T/m$. The number of LEDs L_{m-1} can then be calculated as $L_{m-1} = W_{m-1}/\Delta_{f,m-1} = WT/(m+1)$. Table I lists the results of the LED grouping and frequency allocation scheme. Note that the last group takes the rest of the Mth harmonic range, so the property of the last group is slightly different from that of the previous groups.

From Table I, the number of LEDs that can be supported is

$$\begin{aligned} L &= WT\left(\sum_{m=1}^{M-1}\frac{1}{m+2}+\frac{M}{M+1}\right) \\ &= WT\left(\sum_{m=1}^{M}\frac{1}{m}-\frac{1}{2}\right) \\ &\approx WT\left(\ln M+\gamma-\frac{1}{2}+O(M^{-1})\right) \end{aligned} \tag{40}$$

where the approximation is from [22, chap 1.2, pp.75–79] and $\gamma \approx 0.577$. Hence, the number of LEDs L in this scheme scales logarithmically with M. The numerical values of L are shown in Fig. 9.

Note that there is in practice an upper bound for M due to the same reason in Section III-B. In order to maintain the order $\Delta'_{f,i} = f_{i+1} - f_i > 1/(MT)$ for every i in the presence of offset, we should have a frequency spacing

$$\Delta'_{f,i} \geq \frac{2}{MT} - 2f_{\max}\eta > \frac{1}{MT}. \tag{41}$$

Thus, we have

$$M < \frac{1}{2Tf_{\max}\eta}. \tag{42}$$

When $T = 0.1$, $f_{\max} = 4$ kHz, and $\eta = 100$ ppm, we have $M < 13$ for the proposed allocation scheme.

We can see from Fig. 9 that the number of LEDs achieved is several times smaller than the upper limit obtained in Section III. The performance difference is because we focus on a suboptimum estimation approach, namely the successive estimation, with a low complexity, as will be discussed in more detail in Section IV-D and the Appendix. Associated with this suboptimum estimation approach, we also apply a suboptimum frequency allocation scheme. In the applied frequency allocation scheme, there is a uniform frequency spacing between the LEDs within the same group and the value of the frequency spacing keeps decreasing from Group 1 to M. Whereas in Section III-B, it is shown that the optimum frequency allocation should be in an exponential scale. To be able to attain a performance that is closer to the upper limit, more sophisticated estimation approaches, such as based on maximum likelihood estimation, may be employed, associated with the optimum frequency allocation scheme. However, the computational complexity of such approaches tends to be much higher, especially when the number of LEDs is large.

C. The Component Parameter Estimator

In this section, we present a component parameter estimator that is used in the successive estimation procedure presented earlier in Section IV-B. This component parameter is applied once to each of the M groups. The aim of this estimator is to obtain an estimate $\{\hat{a}_i, \hat{f}_i, \hat{\phi}_i\}$ for each i in every group.

This component estimation procedure can be divided into two steps. By way of illustration, we consider the group $m-1$. In the first step, we estimate the amplitude, frequency and phase of the mth harmonic of each LED, denoted by $\hat{a}_{i,m}$, $\hat{f}_{i,m}$ and $\phi_{i,m}$, respectively. We also know that $\hat{a}_{i,m} = \hat{a}_i b_{i,m}$, $\hat{f}_{i,m} = m\hat{f}_i$, and $\phi_{i,m} - m\phi_i$ is a multiple of 2π such that $-\pi \leq \phi_{i,m} \leq \pi$.

Hence it is straightforward to obtain $\{\hat{a}_i, \hat{f}_i\}$ from $\hat{a}_{i,m}$ and $\hat{f}_{i,m}$. It is however more complicated to obtain $\{\hat{\phi}_i\}$ due to phase ambiguity, which will be resolved in the second step.

1) Obtain $\{\hat{a}_i, \hat{f}_i, \hat{\phi}_{i,M}\}$: As shown in [7], we can design the windowing function $G(f)$ such that $G(m\bar{f}_j - m\bar{f}_i) = 0$, for $i \neq j$, so that ideally we can use $\mathcal{Y}_m(m\bar{f}_i)$ to estimate a_i and $m\phi_i$. In practice, however, due to the existence of frequency offsets, we should in fact use $\mathcal{Y}_m(mf_i)$, instead of $\mathcal{Y}_m(m\bar{f}_i)$. Moreover, there may be some induced interference from $Y_{j,m}(f)$ to the value $\mathcal{Y}_m(mf_i)$, since $mf_j - mf_i$ no longer lies on the zeros of $G(f)$. The resulting estimation error due to these effects of frequency offset is not tolerable, especially because of error propagation in the successive estimation procedure. Thus, due to the induced interference between $Y_{i,m}(f)$ and $Y_{j,m}(f)$, we subtract the interfering $Y_{j,m}(f)$ from $\mathcal{Y}_m(f)$ for the parameter estimation of the ith LED. Further, a more accurate estimation of f_i,

instead of simply using $\bar{f}_i$, is desirable to arrive at better estimation of a_i and ϕ_i, too. To this end, we propose an iterative estimator as given in Algorithm 1.

Algorithm 1: An Iterative Parameter Estimator

1:**for** $i = \mathcal{L}_{m-2}+1$ to $\mathcal{L}_{m-1}$ **do**

2:$\hat{f}_i \leftarrow \bar{f}_i$, $\hat{a}_i \leftarrow |\mathcal{Y}_m(m\hat{f}_i)/b_{i,m}|$

3:$\hat{\phi}_{i,m} \leftarrow \text{angle}(\mathcal{Y}_m(m\hat{f}_i)/b_{i,m})$

4:$\hat{Y}_{i,m}(f) \leftarrow \hat{a}_i b_{i,m} G(f - m\hat{f}_i)\exp(j\hat{\phi}_{i,m})$

5:**end for**

6:**for** N_{iter} iterations **do**

7:**for** $i = \mathcal{L}_{m-2}+1$ to $\mathcal{L}_{m-1}$ **do**

8:$\hat{Y}_{i,m}(f) \leftarrow \mathcal{Y}_m(f) - \sum_j \hat{Y}_{j,m}(f)$, where $|j-i| < L_{\text{neighbor}}$

9:$\hat{f}_i \leftarrow 1/m \arg_f \max |\hat{Y}_{i,m}(f)|$, where $|f - \bar{f}_i| < m\Delta_{f,m-1}/2$

10:$\hat{a}_i \leftarrow |\hat{Y}_{i,m}(m\hat{f}_i)/b_{i,m}|$

11:$\hat{\phi}_{i,m} \leftarrow \text{angle}(\hat{Y}_{i,m}(m\hat{f}_i)/b_{i,m})$

12:$\hat{Y}_{i,m}(f) \leftarrow \hat{a}_i b_{i,m} G(f - m\hat{f}_i)\exp(j\hat{\phi}_{i,m})$

13:**end for**

14:**end for**

The initial value of $\hat{f}_i$ for each i is set to be equal to the ideal frequency $\bar{f}_i$. The initial value of $\hat{a}_i$ and $\hat{\phi}_{i,m}$ are then obtained based on the magnitude and phase of $\mathcal{Y}_m(\bar{f}_i)$. We can also then obtain the initial estimated mth harmonic component $\hat{Y}_{i,m}(f)$ for each i.

In each of the N_{iter} iterations, for the ith LED, we subtract the component $\hat{Y}_{j,m}(f)$ of the neighboring LEDs from $\mathcal{Y}_m(f)$, where $|j-i| < L_{\text{neighbor}}$, since these LEDs give the most significant induced interference to $\hat{Y}_{i,m}(f)$. In practice, it suffices to have $N_{\text{iter}} \leq 5$ and $L_{\text{neighbor}} \leq 10$. The result of this subtraction is considered to be an updated $\hat{Y}_{i,m}(f)$. Then $\hat{f}_i$ is obtained by locating the peak of $|\hat{Y}_{i,m}(f)|$ and $\hat{a}_i$ and $\hat{\phi}_{i,m}$ can in turn be updated based on $\hat{Y}_{i,m}(\hat{f}_i)$.

2) Resolve Phase Ambiguity: In the result of Algorithm 1, besides $\hat{a}_i$ and $\hat{f}_i$, we can obtain $\hat{\phi}_{i,m}$, which could correspond to m possible values $\hat{\phi}_i$, denoted by $\psi_{i,k}$ for $k = 1$ to m, such that $e^{jm\psi_{i,k}} = e^{jm\hat{\phi}_{i,m}}$. This is due to phase ambiguity. This phase ambiguity has to be resolved for the successive estimation procedure since $\hat{\phi}_{i,m+1}$ to $\hat{\phi}_{i,M}$ will be later used for the subtraction steps. To this end, we consider the $(m-1)$th harmonic range of the LEDs in the $(m-1)$th group. Specifically, we consider

$$\begin{aligned}\mathcal{Y}_{m-1}(f) &\approx \sum_{i=\mathcal{L}_{m-2}+1}^{\mathcal{L}_{m-1}} Y_{i,m-1}(f) \\ &= \sum_{i=\mathcal{L}_{m-2}+1}^{\mathcal{L}_{m-1}} a_i b_{i,m-1} e^{j(m-1)\phi_i} \\ &\quad \times G(f-(m-1)f_i). \end{aligned} \tag{43}$$

Theoretically, for every possible $\psi_{i,k}$, we can reconstruct $\hat{Y}_{i,m-1}(f)$. Among these $\{\psi_{i,k}\}$, the one that makes $\hat{Y}_{i,m-1}(f)$ closest to the value of $\mathcal{Y}_{m-1}(f)$ at $f = (m-1)\hat{f}_i$ is taken as $\hat{\phi}_i$. In practice, due to the interference from the neighboring LEDs, we also consider the $(i-1)$th and $(i+1)$th LEDs jointly with the ith LED. Specifically, there are in total m^3 different combinations of $\{\psi_{i-1,k_1}, \psi_{i,k_2}, \psi_{i+1,k_3}\}$, where $k_1, k_2, k_3 \in \{1, 2, \ldots, m\}$.

Let $\mathbf{k} = [k_1, k_2, k_3]$. For every possible $\mathbf{k}$, we can regenerate $\hat{Y}_{l,m-1}(f)$, for $l = \{i-1, i, i+1\}$. The optimal $\mathbf{k}^* = [k_1^*, k_2^*, k_3^*]$ is given by

$$\mathbf{k}^* = \arg_{\mathbf{k}} \min \left| \mathcal{Y}_{m-1}((m-1)\hat{f}_i) - \sum_{l=i-1}^{i+1} \hat{Y}_{l,m-1}((m-1)\hat{f}_i) \right| \tag{44}$$

and the final estimate is obtained as $\hat{\phi}_i = \psi_{i,k_2^*}$. The phase ambiguity is as such resolved.

Finally, note that the mth and $(m-1)$th harmonics of every LED in the $(m-1)$th group should exist for the above described component estimator to work effectively. This gives a minor constraint on the duty cycles. In particular, it is required that each p_i in the $(m-1)$th group has to satisfy that both $|b_{i,m}|$ and $|b_{i,m-1}|$ are larger than δ, where δ is small (e.g., $\delta = 0.001$ is chosen in the numerical results presented in Section V).

D. Complexity Analysis

The computational complexity, in terms of real multiplications, of the proposed successive estimation approach can be shown to be $\sum_{m=1}^{M} \Theta_m$, where Θ_m is given by (46) and (47) in the Appendix. We then compare this complexity with that of the approach in [7]. In the approach in [7], the number of LEDs that can be supported is about $L_0 = 100$. The number of real multiplications is then $\Theta_0 = 4r_{\text{s}}L_0\log_2(2r_{\text{s}}L_0)$, where r_{s} is the oversampling rate as defined in Appendix I. Fig. 10 shows the numerical results for $\sum_{m=1}^{M}\Theta_m/\Theta_0$ for different $L = \sum_{m=1}^{M} L_m$. Here, we assume both approaches use the same $r_{\text{s}} = 10$. It is seen that the complexity increases approximately linearly with respect to the total number of LEDs L.

In particular, to support 500 LEDs with $M = 11$, the total computational complexity the proposed approach in this paper is less than 20 times of that of the individual estimator in [7]. Considering the fact we also support five times as many LEDs as in [7], the computational complexity per LED is only increased by a factor of four, and is thus maintained at a low level.

V. Numerical Results

Due to the large number of possible combinations of $\{p_i, a_i, f_i, \phi_i\}$, it is not possible to show the performance for each parameter set. By way of illustration, we show the case when $p_i = p_{\min}$ for every i, when there is significant signal power in the higher harmonics. Further, we take $a_i = a_k$ for every $i \neq k$, such that every LED receives significant interference from other LEDs. The frequency offsets ϵ_i and ϕ_i are generated randomly, based on uniform distributions, according to 100 ppm clock inaccuracy and $-\pi \leq \phi_i \leq \pi$. Moreover, a triangular windowing function $g(t)$ [7] is applied to the sensor signal.

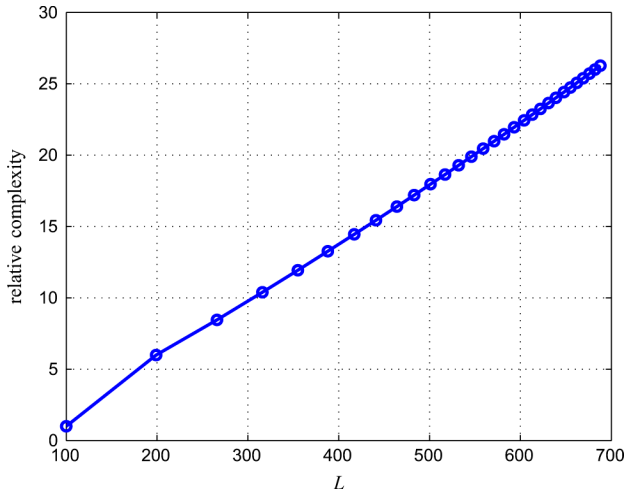

Fig. 10. The relative computational complexity $\sum_{m=1}^{M} \Theta_m/\Theta_0$ for different L. Here in the curve, every bullet corresponds to a value of L prescribed by (40) when M increases from 1 to 30.

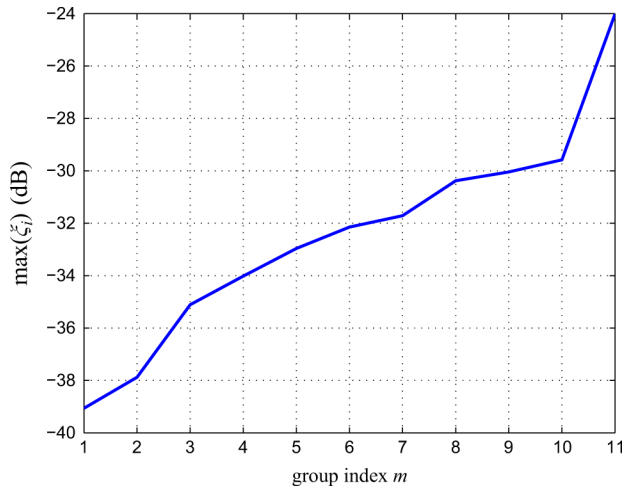

Fig. 11. Estimation performance of each group when $M = 11$, for $L = 500$.

Numerical results are shown in Fig. 11 for $M = 11, L = 501$ and $\zeta_i = 57$ dB. Specifically, the estimation error $\max_i(\xi_i)$ for the LEDs in each group is depicted. Here, the simulations were performed 100 times and the worst case was selected for each $\max_i(\xi_i)$ among the 100 simulation instances. It can be seen that there tends to be a larger error in the later groups than the earlier groups, attributed to error propagation and larger frequency offsets. Nevertheless, the estimation error is well below -20 dB for every LED, as required.

We can further test the performance of the proposed approach for different system parameters. At different SNRs, the estimation performance can also be obtained, as illustrated in Fig. 12. At a lower SNR, the noise introduces a larger estimation error in the groups with a smaller m. This error will further result an even larger error for a larger m due to error propagation. Nevertheless, from Fig. 12, we can obtain adequate estimation performances as long as $\zeta_i > 32$ dB.

The performance of our proposed approach can also be compared with that of the ML estimator that is prescribed by the

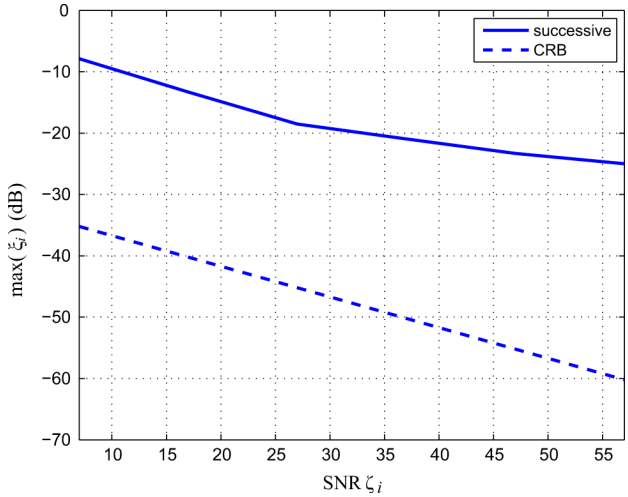

Fig. 12. Estimation performance for different SNR with $M = 11$, $L = 500$, $p_i = p_{\min}$ for each i, and $a_i = a_k$ for $i \neq k$.

CRB analysis in Section III-B. Referring to (21) and replacing L_s by L, we have

$$\hat{\xi}_i = -\frac{1}{2}\zeta_i + 5\log_{10}\frac{p_1(1-p_1)}{4L^2\sum_{k=1}^{m} b_{i,k}^2}, \tag{45}$$

the numerical results of which are also presented in Fig. 12. It can be seen that the performance of the proposed low complexity successive estimation approach, although adequate for the illumination sensing application for $L = 500$, can still potentially be improved significantly by applying more sophisticated approaches such as ML. Moreover, it can be observed that the estimation error in the successive estimation approach does not decrease as quickly as that in the ML estimator, when SNR increases. This is because the performance of the successive estimation approach is also affected by the frequency offsets and error propagation, besides the noise.

In all the presented numerical results, we take $N_{\text{iter}} = 5$ and $L_{\text{neighbor}} = 10$. If we only consider the case $p_i = p_{\min}$ and $a_i = a_k$ for each i and k, we can take smaller values for N_{iter} and L_{neighbor}. However, there are other possible cases, e.g., when a_i and p_i could be quite different for different i. In these cases, the LEDs with a smaller amplitude $a_{i,m}$ may suffer from serious induced interferences from LEDs with a much larger amplitude $a_{k,m}$ where both ith and kth LEDs are in the same LED group. Therefore, the values of $N_{\text{iter}} = 5$ and $L_{\text{neighbor}} = 10$ are taken to give adequate performances also in such cases.

VI. Conclusions and Future Work

We considered the use of multiple harmonics for parameter estimation in illumination sensing for FDM based LED lighting systems. We showed, using the CRB and a frequency error analysis, that a significantly larger number of LEDs can potentially be supported through exploiting multiple harmonics, in comparison to the approach when only the fundamental frequency component is used. Specifically, the number of LEDs can be potentially increased by an order of magnitude. Thereafter, a

successive estimation approach with a manageable computational complexity was presented. With this approach, the number of LEDs that can be supported scales logarithmically with the number of harmonics considered. Simulation results indicate that we can support at least five times the number of LEDs in comparison to the method previously described in [7]. A possible future research direction will be to close the gap between the upper limit on the number of LEDs, and that achieved by the successive estimator, also with a manageable computational complexity. As another future research topic, the results obtained in this paper with the use of a single photosensor can be extended to the case with multiple distributed photosensors, e.g., for the study of illumination sensing for large objects.

APPENDIX
COMPLEXITY ANALYSIS

In the following steps, we discuss the computational complexity of the proposed estimation approach for the parameters $\{\hat{a}_i, \hat{f}_i, \hat{\phi}_i\}$ of the $(m-1)$th group. Here we focus on the complexity of a typical implementation to study the basic properties of the computational complexity. More efficient implementations are beyond the scope of this paper. Moreover, we focus on the number of real valued multiplications, since this operation represents the majority of the computational complexity.

Obtain $Y(f)$: For the estimation of the parameters of the LEDs in the $(m-1)$th group, we need to consider the mth harmonic frequency range with a bandwidth mW_{m-1}, where W_{m-1} is shown in Table I. Assuming a fast Fourier transform (FFT) is used to obtain $Y(f)$, we first need to filter the signal $y(t)g(t)$ and sample the filtered signal with an oversampling rate $r_s \geq 2$. The number of samples is thus $N = Tf_s = Tr_s mW_{m-1} = 2r_s L_{m-1}$. In the frequency domain, we obtain the FFT at N discrete frequency components. Thus, r_s is linearly proportional to the frequency resolution.

Without loss of generality, we assume N to be the power of 2. The number of complex multiplications to obtain $Y(f)$ is then known [23, chap. 9] to be $(N/2)\log_2 N = r_s L_{m-1}\log_2(2r_s L_{m-1}) = r_s \log_2(2r_s)L_{m-1} + r_s L_{m-1}\log_2 L_{m-1}$. Moreover, one complex multiplication can be realized through four[1] real multiplications and two real additions. Thus, the number of real multiplications is $2N\log_2 N = 4r_s\log_2(2r_s)L_{m-1} + 4r_s L_{m-1}\log_2 L_{m-1}$.

Obtain $\mathcal{Y}_m(f)$: To obtain $\mathcal{Y}_m(f)$ as given in (37), we need to subtract from $Y(f)$ the frequency components due to the LEDs in the groups 1 to $m-2$ in the frequency range $(m-1)f_{\max}$ to $m^2 f_{\max}/(m+1)$. The orders of the interfering harmonics are from $m+1$ to $\lfloor 2m^2/(m+1)\rfloor$, where $\lfloor x\rfloor$ denotes the floor of x, i.e., the maximum integer that is not larger than x. Therefore, the corresponding frequency range of the interfering LEDs are $[(m-1)f_{\max}/(m+1), m^2 f_{\max}/(m+1)^2]$, $[(m-1)f_{\max}/(m+2), m^2 f_{\max}/((m+1)(m+2))]$, $\cdots$, $[(m-1)f_{\max}/\lfloor 2m^2/(m+1)\rfloor, m^2 f_{\max}/((m+1)\lfloor 2m^2/(m+1)\rfloor)]$. The number of LEDs in each of these ranges can be obtained easily based on $\{\Delta_{f,m}\}$. The sum of the interfering LEDs in all these regions is the total number of interfering LEDs for the group $m-1$, denoted by K_{m-1}. The value of K_{m-1} can be obtained numerically. For convenience, the value of K_{m-1} is normalized by the value L_{m-1}.

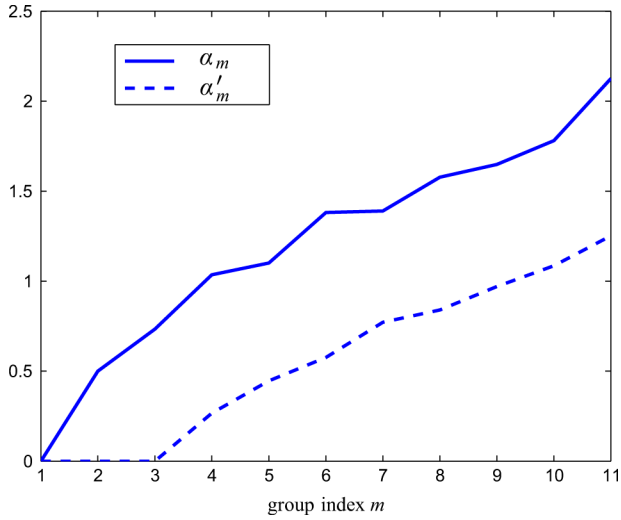

Fig. 13. The number of interfering LEDs for each group, $\alpha_m = K_m/L_m$ and $\alpha'_m = K'_m/L_m$, for $M = 11$.

Let $\alpha_m \triangleq K_m/L_m$. From Fig. 13, the value of α_m is in the range between 0 to 2.5 for $M = 11$. Theoretically, we need to obtain $\hat{Y}_{i,m}(f)$ for any i and m at all the $2r_s L_{m-1}$ discrete frequencies. However, due to limited window length T, for every interfering LED, we only need to consider the frequency range within a few times $1/T$, e.g., $5/T$. Hence, we only need to update $\hat{Y}_{i,m}(f)$ by $2r_s L_{m-1}(5/T)/(mW_{m-1}) = 5r_s$ frequencies. For every frequency, we need to perform two real multiplications. Hence, the total number of real complications in this part is $10r_s K_{m-1} = 10\alpha_{m-1} r_s L_{m-1}$.

Obtain the Initial Estimates $\{\hat{a}_i, \hat{f}_i, \hat{\phi}_{i,m}\}$: As for the steps 1 to 5 in Algorithm 1, the dominant complexity lies in step 4, where the number of real multiplications is $10r_s$ for each LED. The total number of real multiplications in this part is thus $10r_s L_{m-1}$.

Iterative Estimation of $\{\hat{a}_i, \hat{f}_i, \hat{\phi}_{i,m}\}$: Similarly to the above step, the dominant complexity in steps 7 to 15 in Algorithm 1 lies in step 13, where the number of real multiplications is $10r_s$. Hence, the total number of real multiplications in this part is $10N_{\text{iter}} r_s L_{m-1}$.

Obtain $\mathcal{Y}_{m-1}(f)$: For the purpose of resolving the phase ambiguity, we need to obtain $\mathcal{Y}_{m-1}(f)$, see (43), at $\{\hat{f}_i\}$ for every i in group $m-1$. This process is similar to that of $\mathcal{Y}_m(f)$, except that we look at a lower harmonic of the LEDs in group $m-1$. The bandwidth of interest, and the sampling frequency, is thus reduced by a factor of $(m-1)/m$. Therefore, the number of real multiplications to obtain $Y(f)$ equals $(m-1)(4r_s\log_2(2r_s)L_{m-1} + 4r_s L_{m-1}\log_2 L_{m-1})/m$.

Then, the number of computations to subtract the frequency component of the interfering LEDs from other groups is $10r_s K'_{m-1}$, where K'_{m-1} is the number of interfering LEDs

[1]Here, we only consider a straightforward way of implementing the operation of complex multiplication. There exist alternative ways, e.g., to reduce the number of real multiplications to 3 with the cost of more additions, corresponding to one complex multiplication.

in this frequency range and $\alpha'_{m-1} = K'_{m-1}/L_{m-1}$. The numerical values of α'_m are also illustrated in Fig. 13.

The total number of real multiplications in this step is thus $4((m-1)/m)r_{\rm s}\log_2(2r_{\rm s})L_{m-1} + 4((m-1)/m)r_{\rm s}L_{m-1}\log_2 L_{m-1} + 10\alpha'_{m-1}r_{\rm s}L_{m-1}$.

Resolve Phase Ambiguity and Obtain $\{\hat{\phi}_i\}$: The major computations in (44) lie in the computation of $\hat{Y}_{l,m-1}((m-1)\hat{f}_i)$. Basically, for each LED, we need to consider the m possible phases and compute $\hat{Y}_{i,m-1}(f)$ for $f=(m-1)\hat{f}_{i-1}, (m-1)\hat{f}_i$, and $(m-1)\hat{f}_{i+1}$. Hence the number of real multiplications is $6mL_{m-1}$.

The Total Complexity: From the above steps 1) to 6), we can obtain that the total number of real multiplications, denotedy by Θ_{m-1}, in estimating the parameters of the $(m-1)$th group of LEDs is given by

$$\begin{aligned}\Theta_{m-1} &= \left(8-\frac{4}{m}\right) r_{\rm s}L_{m-1}\log_2 L_{m-1} \\ &\quad + 10r_{\rm s}(\alpha_{m-1}+\alpha'_{m-1}+N_{\rm iter}+1)L_{m-1} \\ &\quad + \left(8-\frac{4}{m}\right) r_{\rm s}\log_2(2r_{\rm s})L_{m-1} + 6mL_{m-1}. \quad (46)\end{aligned}$$

Note that, for the last group, i.e., Mth group, we do not have to resolve the phase ambiguity, since the parameters of all the other groups have been estimated. Hence, the corresponding complexity is

$$\begin{aligned}\Theta_M &= \left(8-\frac{4}{M}\right) r_{\rm s}L_M\log_2 L_M \\ &\quad + 10r_{\rm s}(\alpha_M+\alpha'_M+N_{\rm iter}+1)L_M \\ &\quad + \left(8-\frac{4}{M}\right) r_{\rm s}\log_2(2r_{\rm s})L_M. \quad (47)\end{aligned}$$

As a summary, for all the M groups, the number of computations is $\sum_{m=1}^{M}\Theta_m$.

REFERENCES

[1] E. F. Schubert and J. K. Kim, "Solid-state light sources getting smart," *Sci.*, vol. 308, pp. 1274–1278, May 2005.

[2] I. Moreno and C. C. Sun, "Modeling the radiation pattern of LEDs," *Opt. Expr.*, vol. 16, no. 3, pp. 1808–1819, Feb. 2008.

[3] M. Dyble, N. Narendran, A. Bierman, and T. Klein, "Impact of dimming white LEDs: Chromaticity shifts due to different dimming methods," *Proc. SPIE*, vol. 5941, pp. 291–299, 2005.

[4] J.-P. M. G. Linnartz, L. Feri, H. Yang, S. B. Colak, and T. C. W. Schenk, "Code division-based sensing of illumination contributions in solid-state lighting," *IEEE Trans. Signal Process.*, vol. 57, pp. 3984–3998, Oct. 2009.

[5] I. Moreno, C.-Y. Tsai, D. Bermüdez, and C.-C. Sun, "Simple function for intensity distribution from LEDs," *Proc. SPIE*, vol. 6670, 2007.

[6] T. Komine and M. Nakagawa, "Fundamental analysis for visible-light communication system using LED lights," *IEEE Trans. Consum. Electron.*, vol. 50, pp. 100–107, Feb. 2004.

[7] H. Yang, J. W. M. Bergmans, and T. C. W. Schenk, "Illumination sensing in LED lighting systems based on frequency division multiplexing," *IEEE Trans. Signal Process.*, vol. 57, pp. 4269–4281, Nov. 2009.

[8] M. Salsbury and I. Ashdown, "Adapting radio technology to LED feedback systems," *Proc. SPIE*, vol. 6669, 2007.

[9] I. Fryc, S. W. Brown, G. P. Eppeldauer, and Y. Ohno, "LED-based spectrally tunable source for radiometric, photometric, and colorimetric applications," *Opt. Eng.*, vol. 44, no. 11, p. 111 309, Nov. 2005.

[10] N. A. Galano, "Smart Lighting: LED implementation and ambient communication applications," Master's thesis, Univ. Calif., Berkeley, 2009.

[11] D. C. Rife and R. R. Boorstyn, "Multiple tone parameter estimation from discrete-time observations," *Bell Syst. Tech. J.*, vol. 55, no. 9, pp. 1389–1410, Nov. 1976.

[12] P. Stoica, R. L. Moses, B. Friedlander, and T. Soderstrom, "Maximum likelihood estimation of the parameters of multiple sinusoids from noisy measurements," *IEEE Trans. Acoust., Speech, Signal Process.*, vol. 37, pp. 378–392, Mar. 1989.

[13] E. J. Hannan, "The estimation of frequency," *J. Appl. Probabil.*, vol. 10, no. 3, pp. 510–519, Sep. 1973.

[14] B. G. Quinn and E. J. Hannan, *The Estimation and Tracking of Frequency*. Cambridge , U.K.: Cambridge Univ. Press, 2001.

[15] L. B. White, "An iterative method for exact maximum likelihood estimation of the parameters of a harmonic series," *IEEE Trans. Autom. Control*, vol. 38, pp. 367–370, Feb. 1993.

[16] H. Yang, T. C. W. Schenk, J. W. M. Bergmans, and A. Pandharipande, "Parameter estimation of multiple pulse trains for illumination sensing," *Proc. ICASSP*, pp. 3122–3125, Mar. 2010.

[17] H. Meyr, M. Moeneclaey, and S. A. Fechtel, *Digital Communication Receivers: Synchronization, Channel Estimation, and Signal Processing*. New York: Wiley, 1998, ch. 8.

[18] *Digital Addressable Lighting Interfaces (DALI)*, IEC 62386, Jun. 2009.

[19] P. R. Boyce, *Human Factors in Lighting*, 2nd ed. New York: Taylor & Francis, 2003.

[20] G. H. Hardy, J. E. Littlewood, and G. Polya, *Inequalities*, 2nd ed. Cambridge, U.K.: Cambridge Univ. Press, 1988.

[21] D. C. Rife and R. R. Boorstyn, "Single tone parameter estimation from discrete-time observations," *IEEE Trans. Inf. Theory*, vol. 20, pp. 591–598, Sep. 1974.

[22] D. E. Knuth, *The Art of Computer Programming, Volume 1: Fundamental Algorithms*, 3rd ed. Reading, MA: Addison-Wesley, 1997.

[23] A. V. Oppenheim, R. W. Schafer, and J. R. Buck, *Discrete-Time Signal Processing*, 2nd ed. Englewood Cliffs, NJ: Prentice-Hall, 1999.

Hongming Yang (S'06–M'09) received the B.S. and M.S. degrees from the Department of Electronic Engineering, Tsinghua University, Beijing, China, in 2000 and 2003, respectively. He also received the M.E. degree from the Department of Electrical and Computer Engineering, National University of Singapore, Singapore, in 2005. In 2010, he received the Ph.D. degree from the Department of Electrical Engineering, Eindhoven University of Technology (TU/e), Eindhoven, The Netherlands.

He is currently with the Distributed Sensor Systems Department, Philips Research Laboratories, Eindhoven, as a Research Scientist. He was a guest researcher with the same department from 2005 to 2009. His research interest lies in signal processing for illumination systems, digital communications, and recording systems.

Tim C. W. Schenk (S'01–M'07) received the M.Sc. and Ph.D. degrees in electrical engineering from Eindhoven University of Technology (TU/e), Eindhoven, The Netherlands, in 2002 and 2006, respectively.

From 2002 to 2004, he was with the Wireless Systems Research Group, Agere Systems, Nieuwegein, The Netherlands. From 2004 to 2006, he was a Research Assistant with the Radiocommunications Group, TU/e. Currently, he is with Philips Research Laboratories, Eindhoven, as a Senior Scientist and Cluster Leader in the Distributed Sensor Systems department. His research interests include applied signal processing, wireless optical communications, and networked control systems. He authored the book *RF Imperfections in High-Rate Wireless Systems: Impact and Digital Compensation* (The Netherlands: Springer, 2008), and numerous scientific publications in the field of signal processing and communications. He is the inventor of over 40 patents and patent applications.

Dr. Schenk was awarded the 2006 Veder Award from the Dutch Scientific Radio Fund Veder for his contributions in the field of system optimization for multiple-antenna systems.

Jan W. M. Bergmans (SM'91) received the degree of Elektrotechnisch Ingenieur (*cum laude*) in 1982, and the Ph.D. degree in 1987, both from Eindhoven University of Technology, Eindhoven, The Netherlands.

From 1982 to 1999, he was with Philips Research Laboratories, Eindhoven, working on signal-processing techniques and IC-architectures for digital transmission and recording systems. In 1988 and 1989, he was an exchange researcher with Hitachi Central Research Labs, Tokyo, Japan. Since 1999, he has been Professor and Chairman of the Signal Processing Systems Group, Eindhoven University of Technology. Since 1998, he has been an advisor to the Data Storage Institute, Singapore, and since 2000, to Philips Research Laboratories, Eindhoven. He has published extensively in refereed journals, has authored a book, *Digital Baseband Transmission and Recording* (Boston, MA: Kluwer Academic, 1996), and holds approximately 40 U.S. patents.

Ashish Pandharipande (M'03–SM'08) received the B.E. degree in electronics and communications engineering from Osmania University, Hyderabad, India, in 1998, the M.S. degrees in electrical and computer engineering and mathematics, and the Ph.D. degree in electrical and computer engineering from the University of Iowa, Iowa City, in 2000, 2001, and 2002, respectively.

He was a Postdoctoral Researcher with the University of Florida in 2003 and a Senior Researcher with Samsung Advanced Institute of Technology, Suwon, South Korea, from 2004 to 2006. He has held visiting positions with AT&T Laboratories and the Department of Electrical Communication Engineering, Indian Institute of Science, Bangalore, India. He is currently a Senior Scientist with Philips Research, Eindhoven, The Netherlands. His research interests are in the areas of cognitive wireless networks, multicarrier and MIMO wireless communications, sensor signal processing, and system control.

Dr. Pandharipande is currently an editor of EURASIP *JWCN* and was a Guest Coeditor of a Special Issue on Reconfigurable Wireless Systems in *JWCN*. He had served as secretary of the IEEE 802.22 working group on cognitive radio-based regional area networks during 2005–2006.